Size dependent magnetic properties and cation inversion in chemically synthesized $MnFe_2O_4$ nanoparticles

C. N. Chinnasamy,[a] Aria Yang, S. D. Yoon, and Kailin Hsu
Department of Electrical and Computer Engineering, Northeastern University, Boston, Massachusetts 02115

M. D. Shultz and E. E. Carpenter
Department of Chemistry, Virginia Commonwealth University, Richmond, Virginia 23284

S. Mukerjee
Department of Chemistry and Chemical Biology, Northeastern University, Boston, Massachusetts 02115

C. Vittoria and V. G. Harris
Department of Electrical and Computer Engineering, Northeastern University, Boston, Massachusetts 02115

(Presented on 9 January 2007; received 30 October 2006; accepted 28 November 2006; published online 18 April 2007)

$MnFe_2O_4$ nanoparticles with diameters ranging from about 4 to 50 nm were synthesized using a modified coprecipitation method. X-ray diffractograms revealed a pure phase spinel ferrite structure for all samples. Transmission electron microscopy showed that the particles consist of a mixture of both spherical (smaller) and cubic (larger) particles dictated by the reaction kinetics. The Néel temperatures (T_N) of $MnFe_2O_4$ for various particle sizes were determined by using high temperature magnetometry. The ~4 nm $MnFe_2O_4$ particles showed a T_N of about 320 °C whereas the ~50 nm particles had a T_N of about 400 °C. The high Néel temperature, compared with the bulk $MnFe_2O_4$ T_N of 300 °C, is due to a change in cation distribution between the tetrahedral and octahedral sites of the spinel lattice. Results of extended x-ray absorption fine structure measurements indicate a systematic change in the cation distribution dependent on processing conditions. © *2007 American Institute of Physics*. [DOI: 10.1063/1.2710218]

I. INTRODUCTION

The spinel ferrites, MFe_2O_4 (where M=Co, Ni, Mn, Mg, etc.), have value for many technological applications due to their near insulating properties, high permeability, and moderate magnetization. They are used in high frequency transformers, filters, isolators, phase shifters, circulators, and a host of other microwave applications. Recently they have been found utility in biomedical technologies and, in particular, in cancer remediation therapies. Their value in electronics stems in part from the ability to cost effectively produce large quantities of phase pure materials at relatively low temperatures.

The cation distribution in spinel ferrites has been shown to dominate the electrical and magnetic properties.[1] With the advent of nonequilibrium processing and their fabrication as thin films and small particles (often nanoscale), the cation distribution can be modified resulting in inconsistent results. Manganese ferrite ($MnFe_2O_4$) is a well-known microwave ferrite material with a partial inverse spinel structure. Experiments have shown that manganese ferrite bulk material exists with 20% of the Mn cations residing on the octahedral sublattice and 80% on the tetrahedral sublattice.[2]

Earlier work on $MnFe_2O_4$ nanoparticles, which studied the size dependent magnetic properties (5–15 nm particles), suggested that the Néel temperature (T_N) increased with decreasing particle size in a manner consistent with a finite size scaling model.[3] Similar effects have also been observed for the case of ball milled $NiFe_2O_4$ nanoparticles.[4] Some reports show that the cation distribution remained essentially the same in $MnFe_2O_4$ particles of different sizes and indeed the small particles have higher T_N than larger ones.[5] Single phase $MnFe_2O_4$ powders having crystallite sizes ranging between 9.5 and 40 nm have also been obtained by mechanochemical synthesis.[6] The degree of inversion in these samples was found to remain unchanged and independent of size. The Néel temperature was constant irrespective of the particle size. It is clear from these reports that knowledge of the cation distribution of ferrous and nonferrous ions is essential in understanding the magnetic and electronic properties of these materials.

In this study, we report the structural and magnetic properties of $MnFe_2O_4$ nanoparticles with an average particle size between 4 and 50 nm processed by a modified coprecipitation technique. Interestingly, we found that the large 50 nm $MnFe_2O_4$ particles showed higher Néel temperature than the 4 nm ones. The occupancy of Mn ions at octahedral sites was found to greatly influence the Néel temperature.

II. EXPERIMENT

The $MnFe_2O_4$ particle processing experiments were carried out using 0.1M of iron (III) chloride hexahydrate ($FeCl_3 \cdot 6H_2O$, 99%, Sigma Aldrich) and 0.05M of manganese (II) chloride ($MnCl_2 \cdot 4H_2O$, 99%, Sigma Aldrich) dissolved in water with a ratio of $[Fe^{3+}]/[Mn^{2+}]=2:1$. Various mole fractions of $[Me]/[OH^-]$ ranging from 0.45M to 3M were introduced to distilled water and boiled at 98 °C. The mixed

[a]Electronic mail: nchinnas@ece.neu.edu

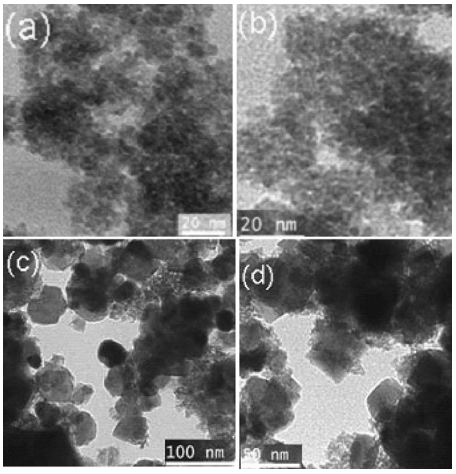

FIG. 1. TEM micrographs of $MnFe_2O_4$ nanoparticles synthesized by using [Fe]/[OH^-] ratios of (a) 4*M*, (b) 2*M*, (c) 1*M*, and (d) 0.425*M*.

metal chloride precursor solution was introduced slowly into the boiling NaOH solution and the reaction was carried out at 98 °C for 120 min. The particles were thoroughly washed several times with distilled water and filtered. The filtered $MnFe_2O_4$ particles were dried at 70 °C for 12 h.

The crystallographic phase of the particles was analyzed using a θ-2θ x-ray powder diffraction (XRD) (Rigaku-Cu $K\alpha$ radiation) technique. The morphology of the particles was examined by transmission electron microscopy (TEM, Hitachi S-4100). Chemical analyses have been carried at using an induction coupled plasma spectrophotometer (ICP 20P VG Elemental Plasma Quad2). The magnetic properties were measured using a vibrating sample magnetometer (VSM, ADE Technologies) from room temperature (RT) to 500 °C. An argon gas atmosphere was used during the thermomagnetic measurements.

Extended x-ray absorption fine structure (EXAFS) data collection was performed using beamline X23B in the National Synchrotron Light Source (NSLS) at Brookhaven National Laboratory (Upton, NY). An energy scan that extended 100 eV below the absorption *K* edge (Mn, 6539 eV; Fe, 7112 eV) and 14 photoelectron wave numbers (i.e., *k*) above the edge was collected in a transmission geometry at room temperature using N_2 gas ionization detectors. The fine structure above the Mn absorption edge was terminated at 12*k* by the appearance of the Fe absorption edge. EXAFS data were analyzed and modeled using the IFEFFIT-based suite of programs, ATHENA and ARTEMIS, developed by Ravel and Newville.[7]

III. RESULTS AND DISCUSSION

Analysis of XRD patterns confirmed the formation of pure single phase $MnFe_2O_4$ particles crystallizing in the cubic spinel structure (Ref. 14). Chemical analysis showed that the samples had the Mn/Fe ratio of 0.5. The as-prepared particles were dispersed either in acetone or water to study the particle size and morphology. The electron microscope studies indicate that the small particles are spherical-like morphology and the larger particles consist of a mixture of both cubic and spherical particles, as shown in Fig. 1. The particle size was varied by controlling the ratio of [Me]/[OH] ion concentration for a fixed reaction time of 120 min at 98 °C.

Figure 2 shows the *M* vs *T* plots of the different particle sizes of $MnFe_2O_4$ determined by using the thermomagnetic measurements with an applied field of 1 kOe. The Néel temperature is found to increase with particle size as shown in Fig. 2 and is significantly higher (400 °C) than the bulk $MnFe_2O_4$ (300 °C). This result is in apparent contradiction to earlier reports that indicated an increase in T_N with reducing particle size and attributed to a finite size scaling.[3] To study the effect of the structural changes in different sized

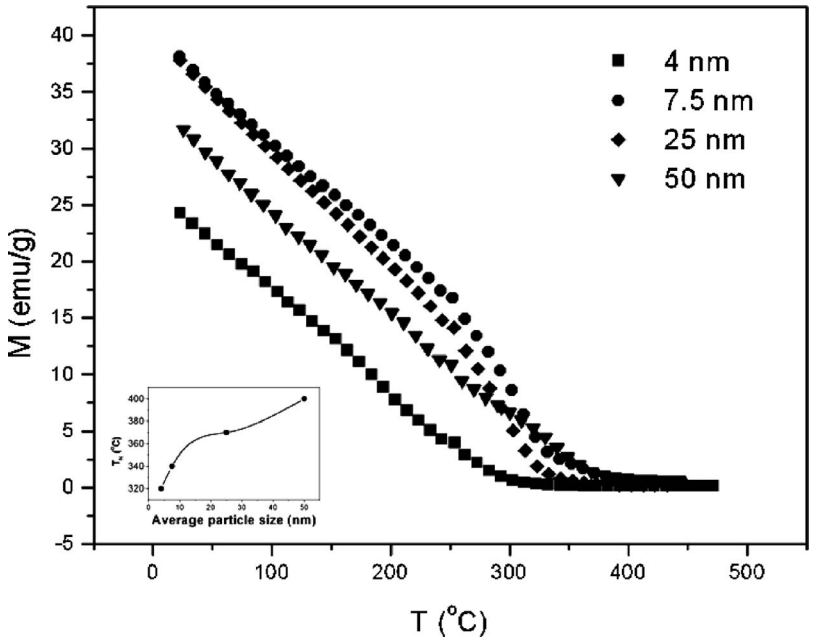

FIG. 2. Magnetization vs temperature data for different sized $MnFe_2O_4$ nanoparticles. Inset figure shows the T_N vs average particle size (continuous line is guide to the eyes).

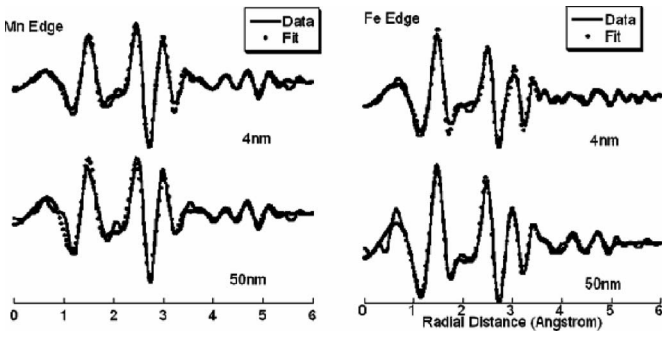

FIG. 3. Real part of Fourier transform of EXAFS data and best fits of manganese edge, and iron edge, for both 4 and 50 nm samples.

$MnFe_2O_4$ nanoparticles, we have carried out preliminary EXAFS measurements for the 4 and the 50 nm samples. Since the cation distribution on the available sites to a large extent decides the magnetic and electric properties of the material, determining the site occupancy is an important step in understanding newly developed ferrites.

The analysis of cation distribution in ferrite materials by EXAFS was performed by Harris *et al.*[8] That analysis was then extended by Calvin *et al.* who performed the multiedge refinement of the spinel structure.[9] Both Harris *et al.* and Calvin *et al.* made use of theoretical standards generated by the FEFF codes of Rehr *et al.*[10] together with the well established EXAFS refinement procedures outlined by Sayers and Bunker.[11] In addition to this approach, we have employed the method described in Ref. 12 by Calvin *et al.* that includes the size of the particle in the EXAFS analysis. In this approach, we assume spherical particles. This is in agreement with the TEM micrographs of Fig. 1 that shows a large portion of the particles exhibit a spherical shape. In this model, the coordination numbers are suppressed relative to a bulk crystal by a factor of

$$1 - \frac{3}{4}\frac{r}{R} + \frac{1}{16}\left(\frac{r}{R}\right)^3,$$

where R is the radius of the particle and r is the distance to the coordination shell in question. The Fourier transform of the EXAFS data provides a real space radial structure function of the environment of the absorbing ion where the absolute amplitude of the function corresponds with the coordination and atomic order of atoms present at the radial distance. In these data, the radial distance corresponds to bond distances that have been shifted in space by a unique electron phase shift which must be calculated from (quasi) first principles and fit to the experimental data. The real part of the Fourier transform of the Fe and Mn EXAFS data for 4 and 50 nm samples and the best fits are shown in Fig. 3. The fit results allow for the determination of cation distribution and a other structure parameters. The R factor, which is a measure of the fractional difference between the fit and the data, is less than 0.03 for both samples. It is calculated that both 4 and 50 nm samples have reduced lattice parameters, 8.42 and 8.37 Å, respectively, in comparison with the bulk value of 8.5 Å. The contraction of the lattice may also increase the Néel temperature for the ~50 nm particles due to the increase of super exchange interaction.[13] Moreover, the percentage of Mn ions on B sites for 4 and 50 nm samples is higher than the 20% typically used as the equilibrium bulk value. The smaller size sample (4 nm) has an inversion parameter of $63\% \pm 1.8\%$ whereas the 50 nm size sample has a value of $51\% \pm 1.9\%$. Here the inversion parameter is the percentage of Mn ions on octahedral sites. In other words, more Fe ions are on octahedral sites in 50 and 4 nm particles than that of the bulk and as a result, it would lead to strengthen the superexchange interaction and hence the higher Néel temperature. Also, the 4 nm $MnFe_2O_4$ particles have a significant fraction of atoms on the surface and their exchange interaction should be weaker due to lower coordination and hence it has reduced Néel temperature (320 °C) compared with the 50 nm ones (400 °C).

ACKNOWLEDGMENTS

This research was supported by the National Science Foundation under Grant No. DMR 0400676 and by the office of Office of Naval Research under Grant No. N00014-05-10349. This research, in part, was performed at the National Synchrotron Light Source (Brookhaven National Laboratory, Upton, NY) which is sponsored by the U.S. Department of Energy.

[1] J. Smith and J. Wijn, *Ferrites* (Cleaver-Hume, London, 1959).
[2] J. M. Hastings and L. M. Corliss, Phys. Rev. **104**, 328 (1956).
[3] J. P. Chen, C. M. Sorenson, K. J. Klabunde, G. C. Hadjipanayis, E. Devlin, and A. Kostikas, Phys. Rev. B **54**, 9288 (1996).
[4] C. N. Chinnasamy, A. Narayanasamy, N. Ponpandian, R. J. Josephus, B. Jeyadevan, K. Tohji, and K. Chattopadhyay, J. Magn. Magn. Mater. **238**, 281 (2002).
[5] G. U. Kulkarni, K. R. Kannan, T. Arunarkavalli, and C. N. R. Rao, Phys. Rev. B **49**, 724 (1994).
[6] M. Muroi, R. Street, P. G. McCormick, and J. Amighian, Phys. Rev. B **63**, 184414 (2001).
[7] B. Ravel and M. Newville, J. Synchrotron Radiat. **12**, 537 (2005).
[8] V. G. Harris, N. C. Koon, C. M. Williams, Q. Zhang, M. Abe, and J. P. Kirkland, Appl. Phys. Lett. **68**, 2082 (1996).
[9] S. Calvin, E. E. Carpenter, V. G. Harris, and S. Morrison, Appl. Phys. Lett. **81**, 3828 (2002).
[10] J. J. Rehr, S. I. Zabinsky, and R. C. Albers, Phys. Rev. Lett. **81**, 3828 (2002).
[11] D. E. Sayers and B. A. Bunker, *X-ray Absorption: Principles, Applications, Techniques of EXAFS, SEXAFS, and XANES* (Wiley, New York, 1998), Vol. 92, pp. 211–253.
[12] S. Calvin, C. J. Riedel, E. E. Carpenter, S. A. Morrison, R. M. Stround, and V. G. Harris, Phys. Scr., T **115**, 744 (2005).
[13] G. A. Samara and A. A. Giardini, Phys. Rev. **186**, 577 (1969).
[14] JCPDS Card No. 10-0319.